

SUMMER STUDENTS PROGRAMM 2008

Measurement of leading neutron production in DIS with H1 detector

Maamuu SOVD

Supervisor: Armen Bunyatyan

Introduction

In ep scattering at HERA, hadronic correlations in the proton in form of virtual pions are believed to play an important dynamical role in the nucleon structure. The proton might fluctuate into a state consisting of a pion and a neutron ($p \rightarrow n\pi^+$). Numerous theoretical works have suggested, that the production of highly energetic, forward neutrons in deep - inelastic ep scattering is sensitive to the structure of pion for which our knowledge from fixed target experiments is limited to high x values.

We use the kinematic variables x , Q^2 , and y to describe the inclusive DIS scattering process. They are defined as:

$$x = \frac{-q^2}{2p \cdot q}, \quad Q^2 = -q^2, \quad y = \frac{p \cdot q}{p \cdot k} \quad (1)$$

where p , k and q are the four - momenta of the incident proton, the incident positron and the exchanged virtual photon coupling to the positron. At the ep center - of - mass energy \sqrt{s} they are related by $Q^2 = sxy$.

The kinematic variables used to describe a final state neutron are:

$$\begin{aligned} t &= (p - p')^2 \simeq -\frac{p_T^2}{x_L} - (1 - x_L) \left(\frac{m_n^2}{x_L} - m_p^2 \right) \\ x_L &= 1 - \frac{q \cdot (p - p')}{q \cdot p} \simeq \frac{E'}{E_p} \end{aligned} \quad (2)$$

where p' is the four - momentum of the final state neutron, m_n is the mass of the neutron and m_p is the proton mass. As defined, t corresponds to the squared four - momentum transferred between the incident proton and the final state neutron.

The data were taken during 2006 - 2007 using the HERA accelerator at Deutsches Elektronen - Synchrotron (DESY) where 27.5 GeV positrons collided with 920 GeV protons. The total luminosity of the sample used in this analysis is 121.6 pb^{-1} . The aim of this work is further investigation of the properties of events with leading neutrons and tests of the consistency of the pion exchange picture of leading neutron production. At this stage of project the goal was to select the DIS events containing leading neutron from the H1 data and compare the basic distributions with the Monte Carlo simulation based on pion exchange model.

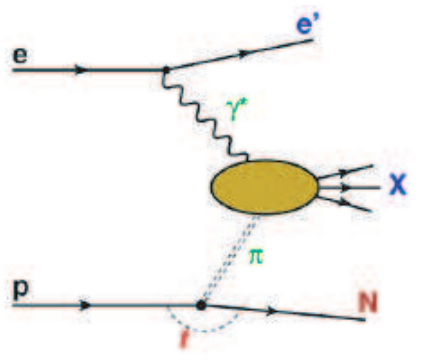


Figure 1: Schematic diagram of deep inelastic electron-proton scattering with leading neutron in final state

RAPGAP 3.1 program is used to generate the pion exchange process. In this model, the incident proton is split into a neutron and π^+ , which then undergoes a DIS interaction.

The cross - section of electron - proton scattering takes the form

$$d\sigma(ep \rightarrow nX) = f_{\pi^+/p}(x_L, t) \cdot d\sigma(e\pi^+ \rightarrow X) \quad (3)$$

where $f_{\pi^+/p}(x_L, t)$ represents the pion flux associated with the beam proton and $d\sigma(ep\pi^+ \rightarrow X)$ is the cross section of the electron - pion interaction. The pion flux factor is taken from the light - cone representation

$$f_{\pi^+/p}(x_L, t) = \frac{1}{2\pi} \frac{g_{p\pi N}^2}{4\pi} (1 - x_L) \frac{-t}{(m_\pi^2 - t)^2} \exp\left(-R_{\pi n}^2 \frac{m_\pi^2 - t}{1 - x_L}\right) \quad (4)$$

where m_π is a pion mass, $g_{p\pi n}^2/4\pi = 13.6$ is the $p\pi n$ coupling constant known from phenomenological analyses of low - energy data.

Detector:H1 and FNC

The H1 Detector

The central ep interaction region of H1 detector is surrounded by two large concentric drift chambers (CJCs), operated inside a 1.16 T solenoidal magnetic field. Charged particles are measured in the pseudorapidity range $-1.5 < \eta < 1.5$ with a transverse momentum resolution of $\sigma(P_T)/P_T \simeq 0.005 P_T / \text{GeV} \oplus 0.015$. Two additional drift chambers (CIZ, COZ) complement the CJCs by precisely measuring the z coordinates of track segments and hence improve the determination of the polar angle. Multi-wire proportional chambers (MWPC) provide fast signals for triggering purposes.

A finely segmented electromagnetic and hadronic liquid argon calorimeter (LAr) covers the range $-1.5 < \eta < 3.4$. The energy resolution is $\sigma(E)/E = 0.11/\sqrt{E/\text{GeV}}$ for electromagnetic showers and $\sigma(E)/E = 0.50/\sqrt{E/\text{GeV}}$ for hadrons. A lead/scintillating fibre calorimeter (SpaCal) covers the backward region $-4 < \eta < -1.4$.

The data sample of this analysis was collected using a trigger which requires the scattered position to be measured in the SpaCal, at least one high transverse momentum track to be reconstructed in the central tracking chambers and an event vertex to be identified by the MWPCs.

The FNC detector

To measure the forward neutrons, the H1 experiment has installed the Forward Neutron Calorimeters (FNC). It was installed at $\theta = 0$ deg and at 106 m from the interaction point in the proton beam direction. The detectors are about 2m long with $\sim 70 \times 70 \text{ cm}^2$ transverse size.

The general view of the H1-FNC is shown in Fig.2. It consists of the Main Calorimeter and the Preshower. In addition, two layers of veto counters situated at the distance of 2 m in front of Preshower are used to veto charged particles. The Preshower, installed in front of the Main calorimeter, is $\sim 40\text{cm}$ ($\sim 1.5\lambda$) long lead-scintillator sandwich calorimeter. The energy resolution for electromagnetic showers is $\sim 20\%/\sqrt{E [\text{GeV}]}$ and the spatial resolution is $\sim 2 \text{ mm}$. The Preshower provides also efficient separation of electromagnetic and hadronic showers.

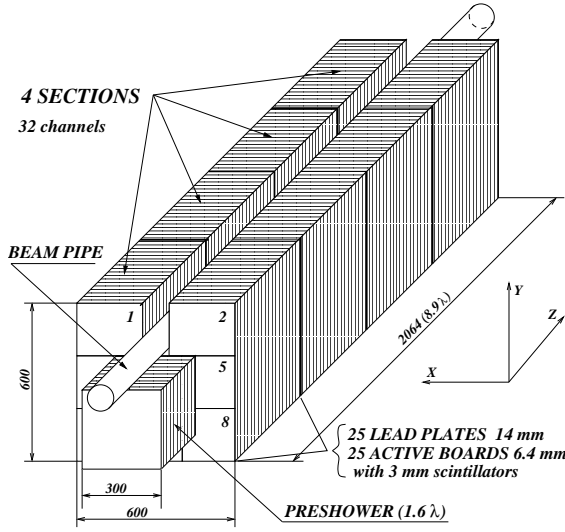


Figure 2: General view of the H1-FNC calorimeter

The Main Calorimeter of H1-FNC is a sandwich-type calorimeter consisting of four identical sections with transverse dimensions $60 \times 60 \text{ cm}^2$ and 51.5 cm long. Each section consists of 25 lead absorber plates 14 mm thick, and 25 active boards with 3 mm scintillators. The total length of the Main calorimeter is 206.5 cm.

The energy response of the H1-FNC calorimeter is linear up to 3% precision and the energy resolution is

$$\sigma_E/E = \left(\frac{63.4 \pm 4.7}{\sqrt{E[\text{GeV}]}} \oplus (3.0 \pm 0.4) \right) \%.$$

Event selection

The analysis uses the data sample collected in electron - proton in 2006-2007. Events were triggered by combinations of the SPACAL electron and Forward Neutron Calorimeter (FNC) triggers. The total integrated luminosity of the data sample is 121.6 pb^{-1} and Monte Carlo RAPGAP 3.1 is 204.84 pb^{-1} . The MC file contains 7000000 events. Analysis is done in H1oo 3.3.8 framework.

Events with leading neutron are selected by requiring the energy in FNC to be above 200 GeV within the acceptance region.

Further cuts are applied to ensure the quality of the data and to remove non-DIS events: the event vertex is required to be within 35 cm of the nominal interaction point. The energy from the angle of scattered electron are required to be $E_e > 11 \text{ GeV}$ and $150^\circ < \theta_e < 180^\circ$, respectively. Furthermore, events are selected within the DIS kinematic ranges $5 < Q^2 < 100 \text{ GeV}^2$ and $0.02 < y < 0.6$. The selection criteria are described in Table 1. After all selection the final data sample contains 265313 events (from total 240 millions).

Results and Summary

The comparison of distributions for the data and Rapgap simulation is shown in Figs.6-12. The distributions are shown for the event z-vertex, scattered electron energy and angles, the energy, angles, transverse momentum and the coordinates of neutron candidate in FNC detector.

As seen from the figures, in general, the Rapgap Monte Carlo which includes pion exchange gives good description of the data distributions.

Table 1: Event selection criteria

$30\text{GeV} < E(Pz) < 75\text{GeV}$
$-50\text{cm} < VtzZ < 50\text{cm}$
$0.02 < Yav < 0.61$
$0 < ElectronRaduis < 75\text{cm}$
$0.22 < FNCx_L = E_{FNC}/920. < 1.02$
$0 < p_{T,n} < 0.7\text{GeV}$
$0 < p_{T,n}^2 < 0.5\text{GeV}$
$0 < \theta_{FNC} < 0.8\text{mrad}$
$-9\text{cm} < FNCx_{all} < 3\text{cm}$
$-3\text{cm} < FNCy_{all} < 7\text{cm}$

Table 2: The dependence of number of events selected in this analysis and the event Run number

event count	runno	eveno
10000	473124	3733
20000	474863	225183
30000	476326	518
40000	477669	133933
50000	478936	81406
60000	480010	40884
70000	481051	340936
80000	482656	193975
90000	483831	127937
100000	484883	81976
110000	485824	256777
120000	486724	36515
130000	487949	133416
140000	488735	173134
150000	489539	1160
160000	491058	164105
170000	491801	222331
180000	493274	60727
190000	493953	235638
200000	494968	16546
210000	496552	104347
220000	497530	170
230000	498063	274998
240000	498827	330923
250000	499574	207800
260000	500268	64967

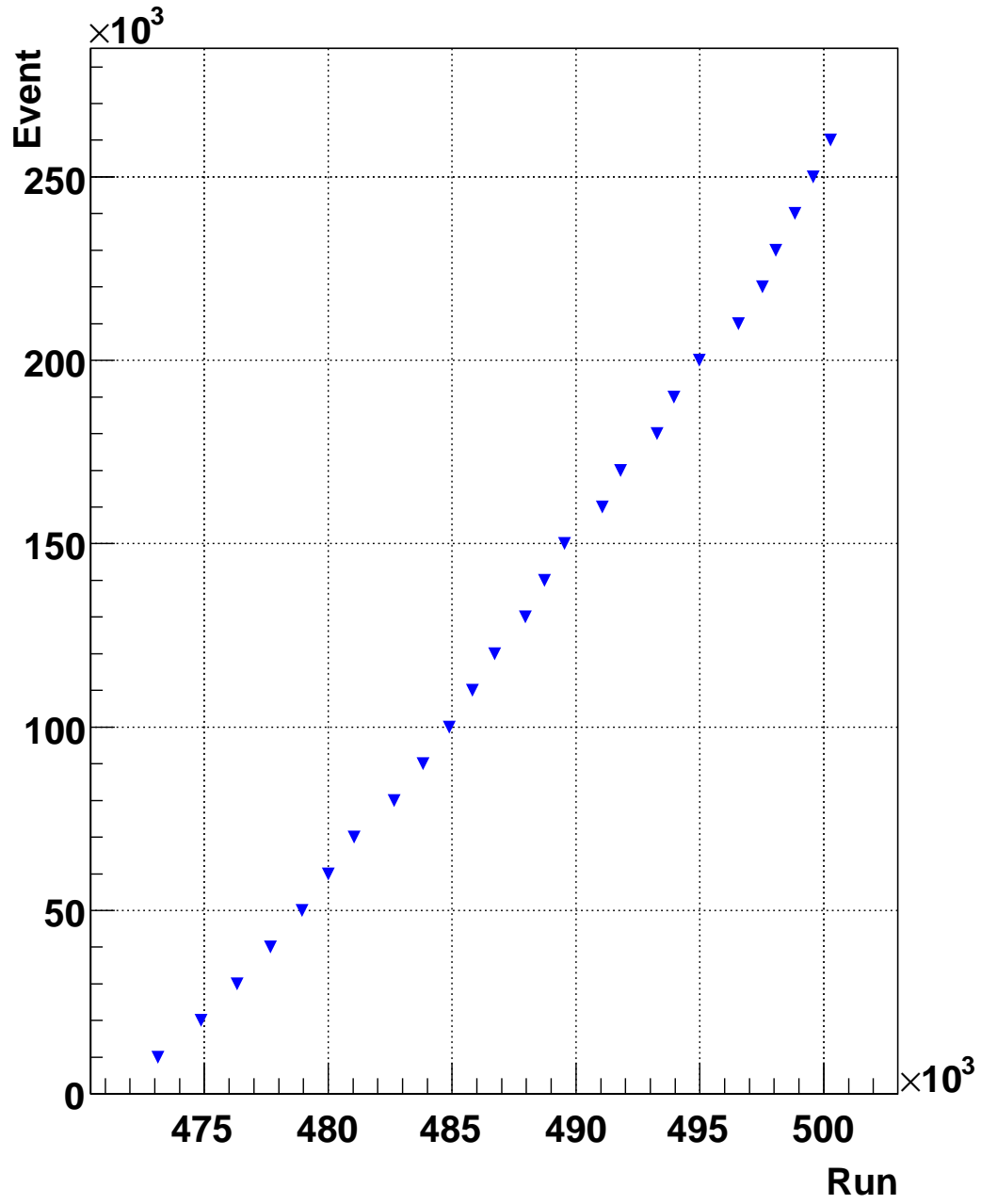


Figure 3:

Figure 4: The dependence of number of events selected in this analysis and the event Run number

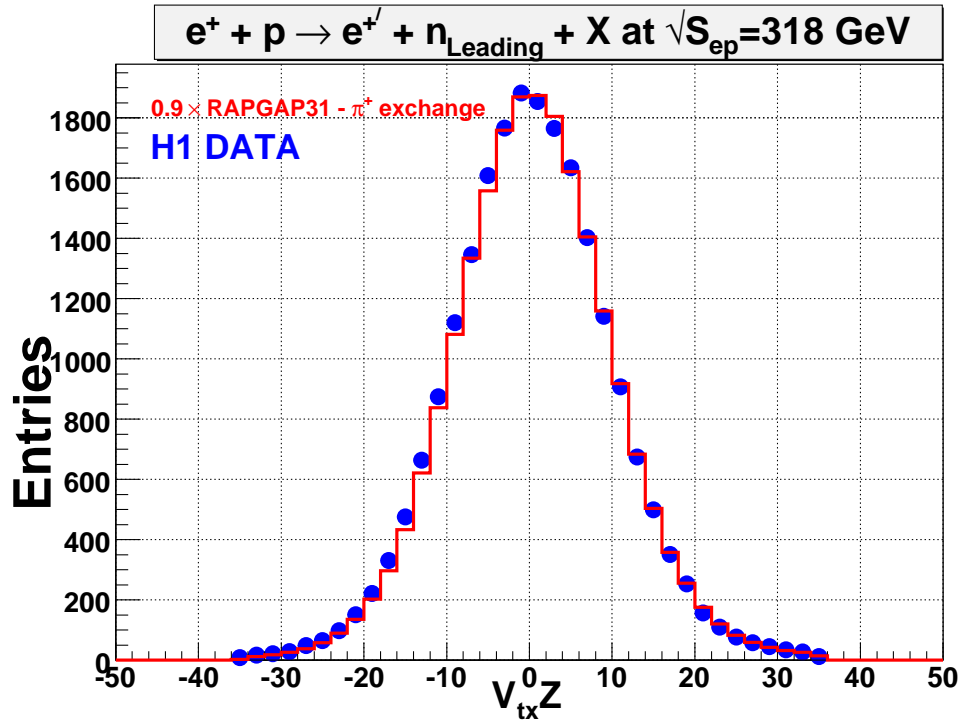


Figure 5: z position of interaction vertex for deep inelastic scattering events with leading neutron

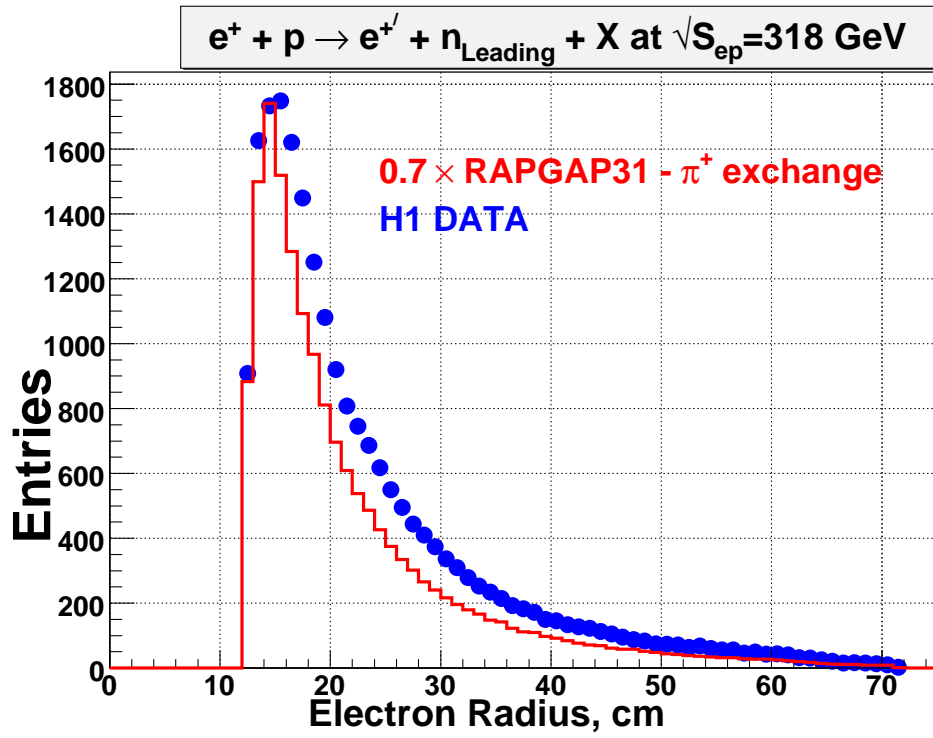
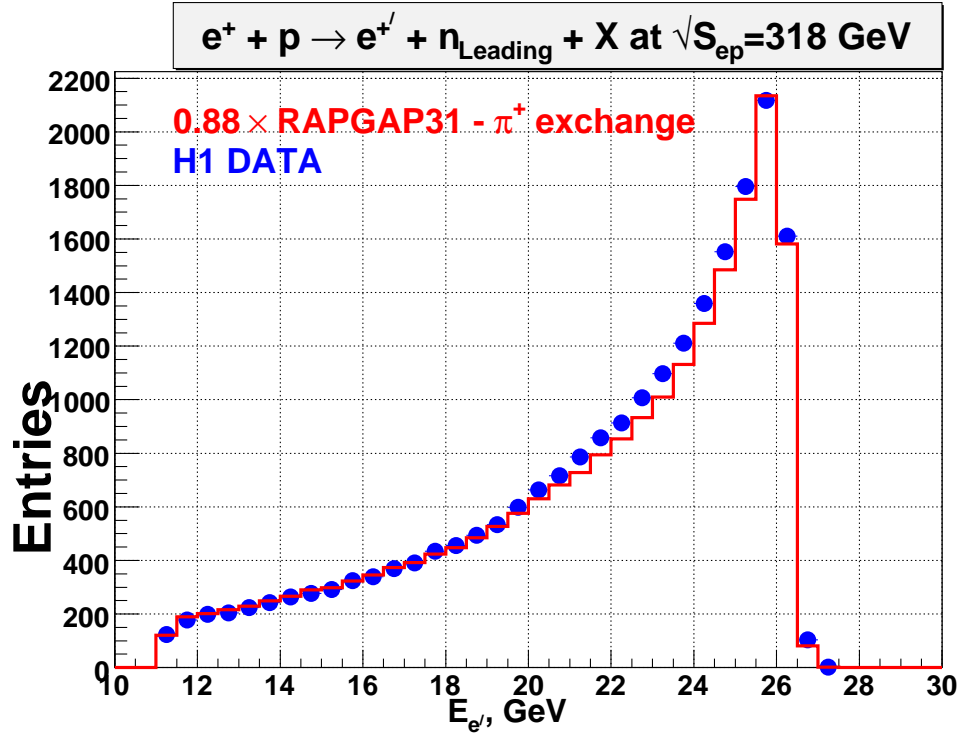


Figure 6: The distribution of the scattered electron energy $E_e > 11\text{GeV}$ and electron radius for deep inelastic scattering events with leading neutron

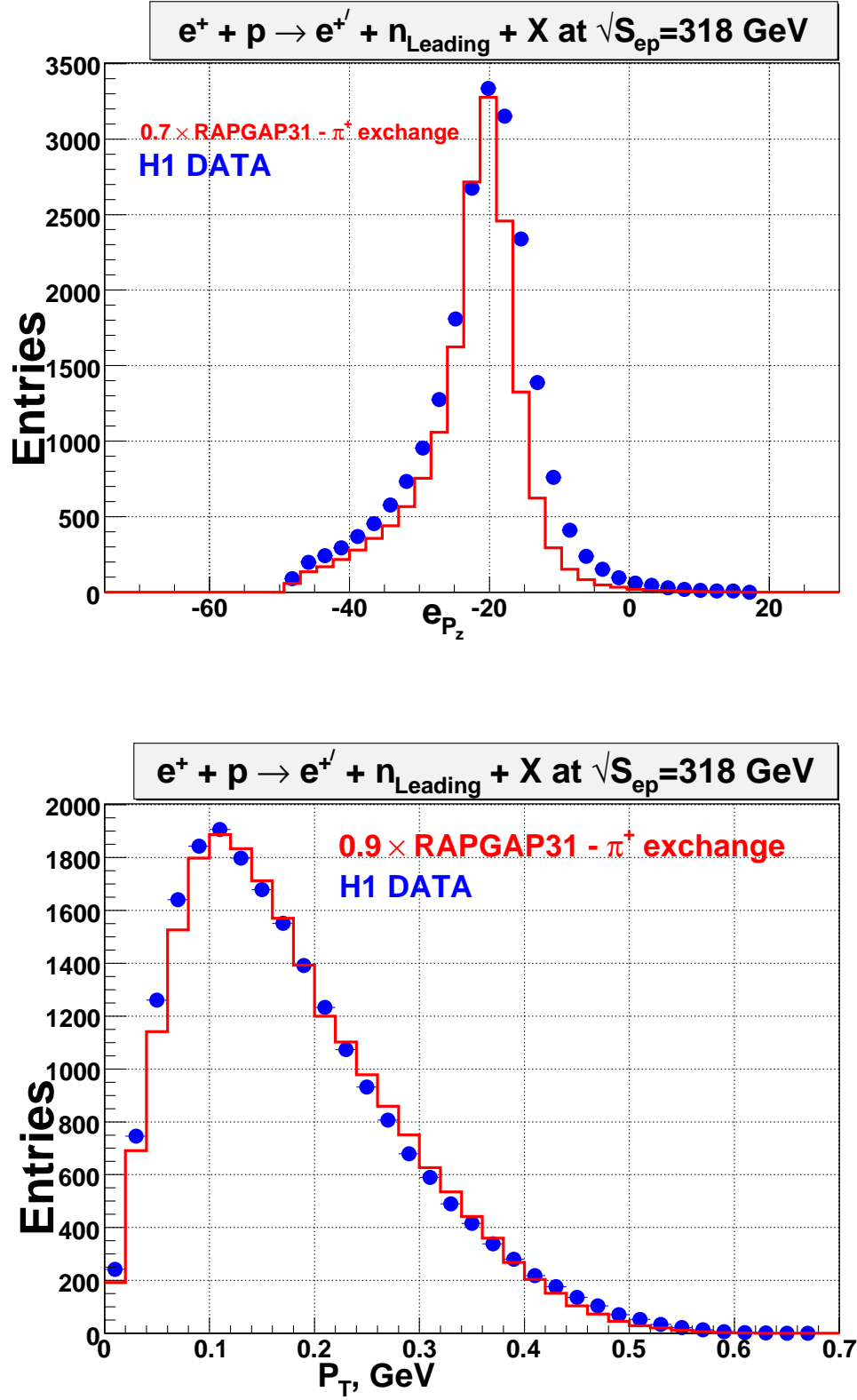


Figure 7: $\sum E - P_z$ and p_T distributions for deep inelastic scattering events with leading neutron

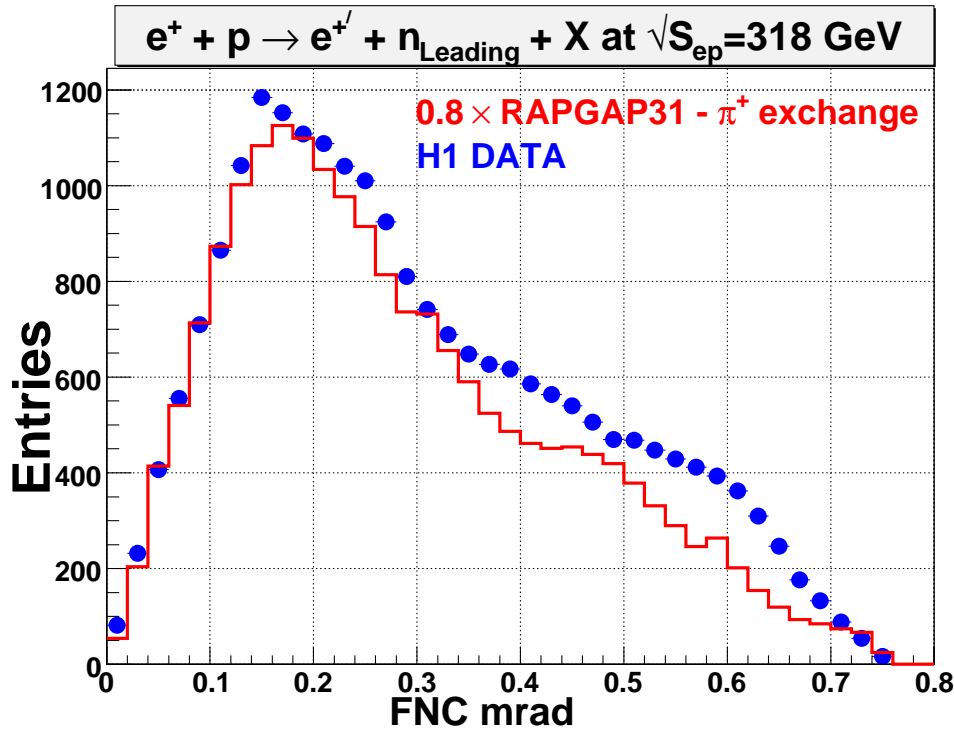
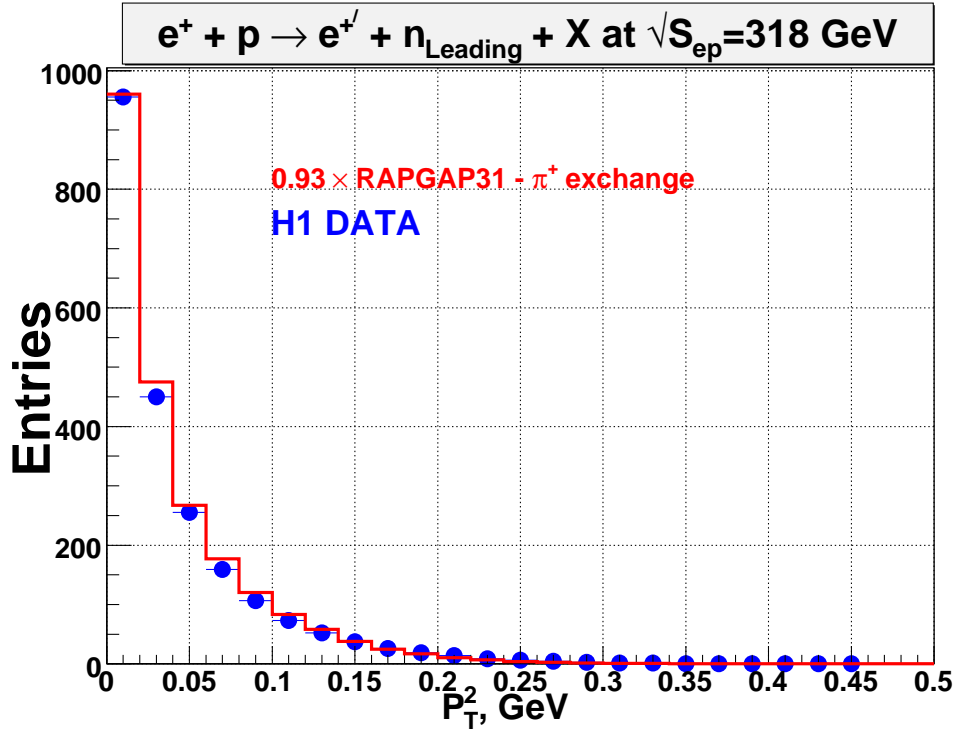


Figure 8: The p_T^2 and θ distributions for leading neutrons in deep - inelastic scattering

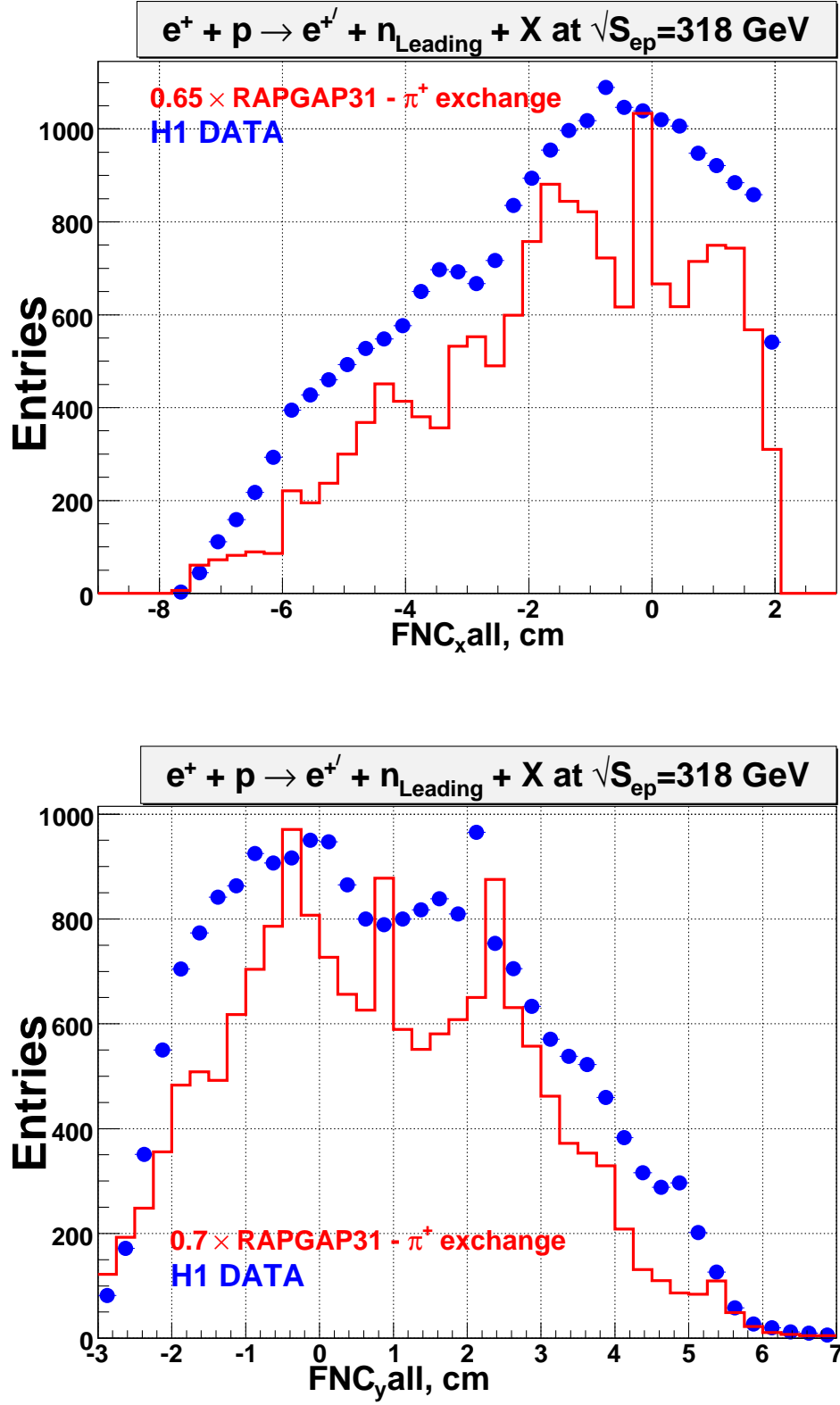


Figure 9: Distributions of FNC x and y coordinates for leading neutron, in DIS events

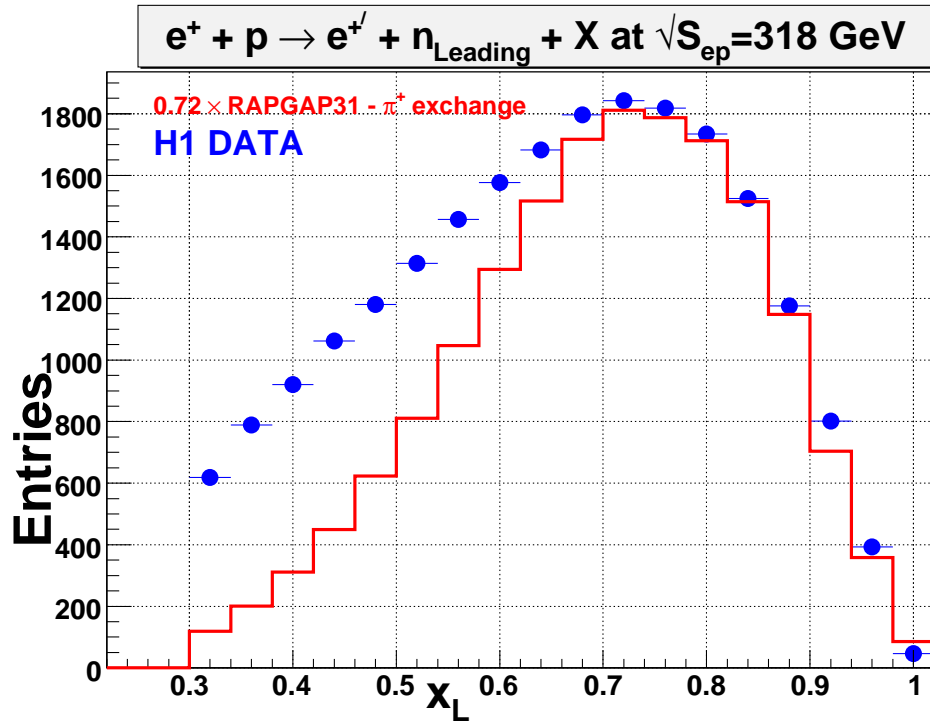


Figure 10: The x_L distribution in deep inelastic scattering with leading neutron

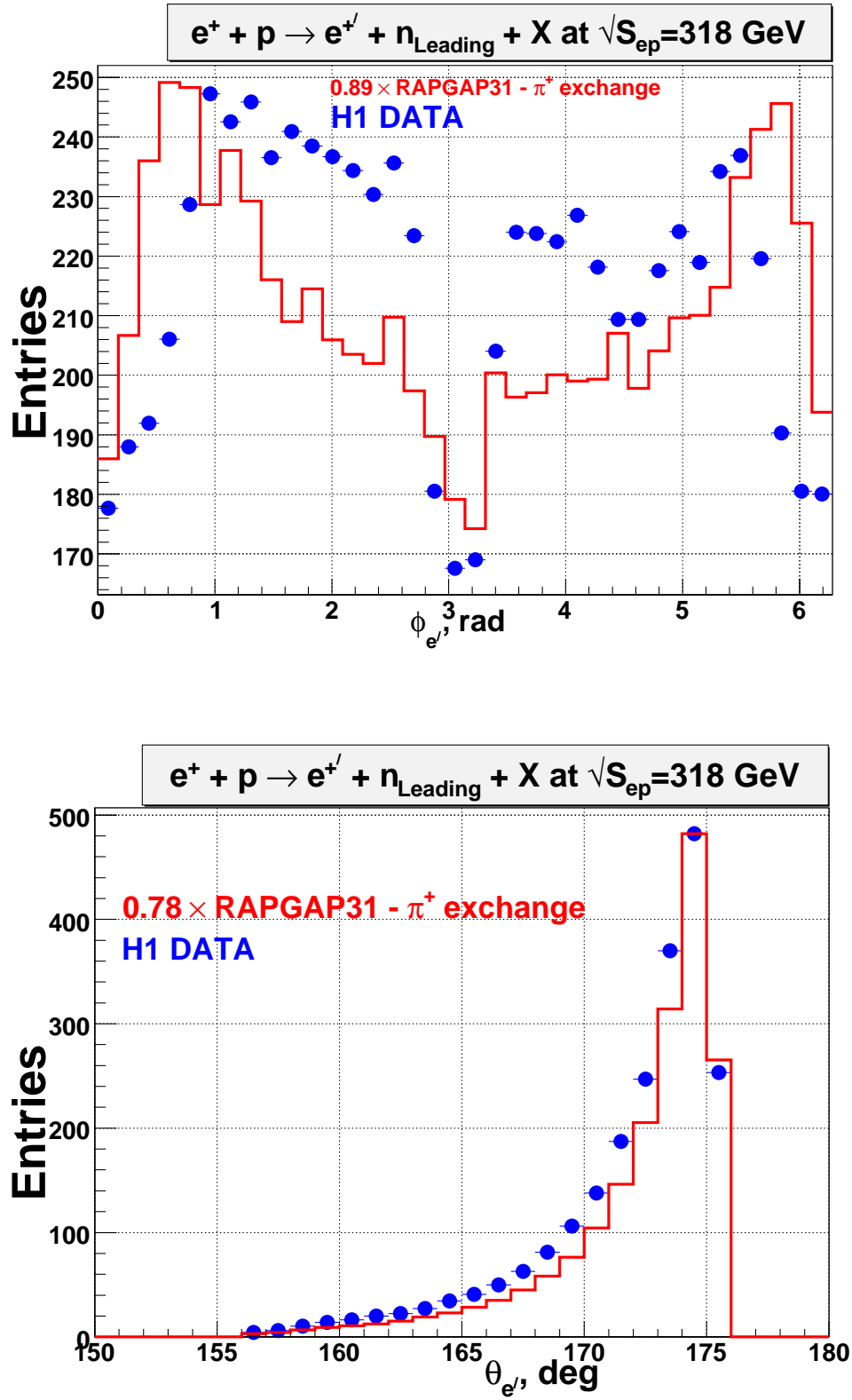


Figure 11: Scattering electron angle ϕ and θ for deep inelastic scattering events with leading neutron

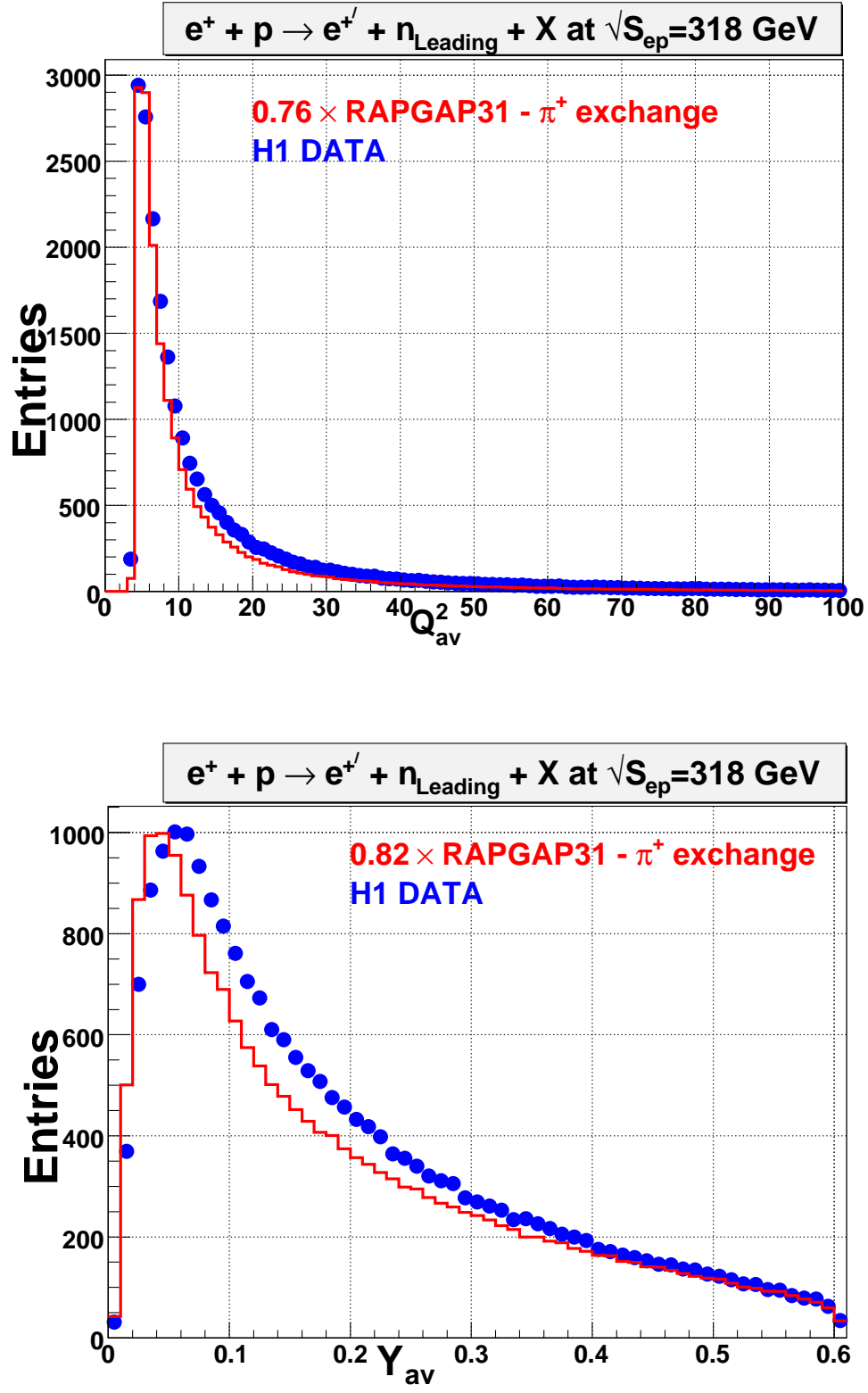


Figure 12: Q^2 and y distributions in deep inelastic scattering with leading neutrons